buildings

MDPI

Article

In Situ Testing Evaluation and Numerical Simulation of CFRP-Strengthened Reinforced Concrete Two-Way Slab with Initial Defect

Yepu Sheng and Yu Gong *

School of Civil Engineering, Shandong Jianzhu University, Jinan 250101, China; shengyepu@live.com
* Correspondence: gysdjzu@163.com

Abstract: Carbon fiber-reinforced polymer (CFRP) composites, renowned for their high strength-to-weight ratio, are increasingly utilized in the strengthening of structural components. The application of CFRP for strengthening concrete components notably improves the cracking moment and substantially elevates the ultimate load-bearing capacity. This study focuses on a reinforced concrete (RC) two-way slab with an initial defect, specifically an initial deflection. To avert deformations or damages that could break structural integrity during service, the slab was strengthened by adhering CFRP to its underside. An in situ multi-stage loading test was conducted to evaluate the load-bearing capacity of the CFRP-strengthened slab, and the findings revealed that the mid-span deflection of the two-way slab incrementally reached 1.64 mm after the loading stages, with no observable signs of concrete cracking, debonding, or tearing of the CFRP-strengthened slab. The failure modes indicated a transition from concrete compression damage to CFRP anchorage stress concentrations, highlighting the effective stress distribution and load-sharing synergy provided by CFRP-strengthening. Additionally, a numerical model based on the finite element (FE) method was developed using ABAQUS to simulate the component's performance during the loading process. A comparison between the measured mid-span deflection of the strengthened slab and the numerically simulated values confirmed the high accuracy and rationality of the simulation method. Utilizing the validated numerical model, an analysis of the slab's ultimate load capacity was conducted, demonstrating that the CFRP strengthening technique effectively increased the load-bearing capacity of the initially imperfect RC two-way slab by nearly 50%.

Keywords: two-way slab; initial deflection; loading experiment; bearing capacity; CFRP

check for updates

Academic Editor: Paulo Santos

Received: 16 December 2024
Revised: 25 December 2024
Accepted: 26 December 2024
Published: 30 December 2024

Citation: Sheng, Y.; Gong, Y. In Situ Testing Evaluation and Numerical Simulation of CFRP-Strengthened Reinforced Concrete Two-Way Slab with Initial Defect. *Buildings* **2025**, *15*, 82. https://doi.org/10.3390/buildings15010082

Copyright: © 2024 by the authors. Licensee MDPI, Basel, Switzerland. This article is an open access article distributed under the terms and conditions of the Creative Commons Attribution (CC BY) license (https://creativecommons.org/licenses/by/4.0/).

1. Introduction

Slabs serve as crucial horizontal support and connect elements in a floor system, bridging walls and columns. As structural components are primarily designed to bear and transfer vertical loads from the floor, reinforced concrete (RC) slabs must satisfy stringent criteria for load-bearing capacity, deformation, and serviceability throughout their operational lifespan [1]. The predominant bending stresses in RC slabs can intensify load effects, substantially reducing the structural capacity and durability when faced with initial defects such as deflection or cracking. These defects, which may emerge during construction or regular use, pose a significant threat to the integrity and safety of high-rise building structures.

Currently, the application and research on the strengthening of RC slabs both domestically and internationally primarily draw on the operational modes of structural components

such as beams and columns. Common strengthening methods include the use of shear studs, fiber-reinforced polymers (FRPs), and textile-reinforced mortar (TRM) [2,3]. To predict the bearing performance and strengthening effects of the strengthened RC two-way slabs, in situ loading tests under specific conditions and sophisticated numerical simulation techniques are necessary. Unlike the common strengthening schemes for beams and columns, such as increasing cross-sectional areas, external reinforcement, and adding energy-dissipating components, the strengthening and retrofit design of two-way slab structures often employ materials with a higher elastic modulus and tensile strength, such as bonded steel plates and carbon fiber-reinforced polymer (CFRP). This strengthening method can be naturally completed in situ without causing damage to the original structure and without significantly increasing the size of the component [4,5]. The strengthening method using metal plates has good applicability and workability, providing effective strengthening for various structural component forms. However, during the load-bearing process, high demands are placed on the anchorage of the steel plates and the quality of their bonding. For components with initial defects or irregular, uneven sections, this method may struggle to achieve the reliable adhesion of steel or aluminum plates, leading to suboptimal strengthening effects and underutilization of the performance advantages of metal materials [6–8]. In contrast, the use of high-performance carbon fiber materials significantly improves and enhances the bearing performance of two-way slabs [9,10]. CFRP, known for its high strength and efficiency, excellent impact and fatigue resistance, and superior corrosion resistance [11–14], has been shown in studies to achieve good adhesion to concrete with reliable load-sharing synergy. However, due to the high strength and extremely thin profile of CFRP sheets, they are prone to brittle damage during strengthening and construction operations [15–17].

Recent studies have significantly contributed to the understanding of the CFRP-strengthened effects on RC slabs. Al-Rousan et al. [18] demonstrated that CFRP-strengthening, particularly in unidirectional sheet form, enhances flexural strength while maintaining ductility. Santos et al. [19] showed that CFRP systems, including the stitch and embedding through section (ETS) methods, effectively increase punching shear strength. Breveglieri and Czaderski [20] found that CFRP strips' long-term performance is resilient to thermal cycles and sustained loads, with adhesive viscoelasticity being a key service factor. Al-Rousan et al. [21] emphasized the importance of anchorage systems in CFRP strengthening to prevent debonding and optimize load-carrying capacity. Ghayeb et al. [22] confirmed that CFRP sheets significantly boost two-way RC slabs' punching shear resistance, with their analytical model aligning with existing standards, aiding in the design and assessment of strengthened slabs. Lastly, Zhou et al. [23] introduced a self-locking hybrid anchoring technique for CFRP sheets in one-way RC slabs, showing improved debonding resistance and strengthening efficiency, which is crucial for enhancing the reliability and durability of CFRP-strengthened RC elements. In parallel, the referenced articles [24–28] explore the specific advancements and challenges associated with the use of CFRP and glass fiber-reinforced polymer (GFRP) in strengthening structures. The study by Li [24] introduced a wedge-shaped bond anchorage system for pultruded CFRP plates, emphasizing its effectiveness in uniformly distributing shear stress and reducing stress concentration, significantly enhancing anchorage efficiency and the overall performance of CFRP-strengthening systems. As for the influence factors, Ke et al. [25] provided a comprehensive review of the influence of environmental factors such as temperature, moisture, and corrosion on bond performance, as well as underscoring the importance of adhesive properties and joint geometry in enhancing durability and effectiveness. Complementing the body of research on CFRP-strengthening, Xian et al. [26,27] provided a thorough evaluation of the mechanical properties of GFRP composites across a range of conditions. It reported the

long-term performance of GFRP over thermosetting composites. These studies, through comparative analysis and leveraging their strengths, collectively highlight the multifaceted advantages of CFRP in RC slab strengthening, from immediate strength gains to long-term durability and performance under various conditions.

In summary, research outcomes have been achieved based on the in situ testing of reinforced concrete, full-scale component testing, and load-bearing capacity tests of scaled components for strengthening effects. However, to study and evaluate the strengthening effects throughout the entire load-bearing process, sophisticated numerical simulation based on the finite element (FE) method is required. Previous studies [29–33] have provided a new perspective for strengthening research and the effective evaluation of structures. A study by Shu et al. [34] analyzed two-way RC slabs under bending through nonlinear finite element analysis, examining the impact of various modeling parameters on the prediction accuracy of load-carrying capacity, load–deflection curve response, and crack patterns. Xu et al.'s theoretical calculations [35], complemented by experimental evidence, quantified the influence of bonding layers on the flexural strengthening of RC slabs with CFRP sheets. Sharaky et al. [36] conducted a FE model to predict the slabs' behavior, offering insights into the effects of bond length, material properties, and strengthening area on the strengthening outcomes. Zou et al. [37] simulated the fatigue behavior of RC beams strengthened with side-bonded CFRP, demonstrating its effectiveness in predicting the fatigue performance of CFRP-strengthened beams and providing a basis for predicting their fatigue life under different loading conditions.

The subject of this study is an RC two-way slab component located in an existing 34-story residential building. The component exhibited an initial deflection due to the influence of curing, environmental factors, and construction loads. To prevent unexpected damage and interaction effects during subsequent operations, the authors' team conducted in situ strengthening measures prior to the normal use phase of the structure. This paper investigated the application and performance enhancement achieved by using bonding CFRP in situ as a strengthening method. A multi-stage loading test, designed to the permissible load-bearing capacity level, was employed to measure the performance of the strengthened component and to study the distribution regulation of stress and strain. A FE model was established and calibrated based on field measurement data, and the model was applied to analyze and predict the ultimate load-bearing capacity of the element.

2. Project Overview and Test Plan

2.1. Project Information

This study concerns a high-rise residential building, designed and completed in 2016, that is located in northern China and features a structural system of frames and shear walls. The focus is on a RC slab that exhibits mid-span deflection, with dimensions of 4100 mm × 5900 mm × 160 mm. The slab is reinforced with double-layer, two-way CRB600H rebars of Φ 6 at 150 mm spacing, and the concrete grade is C25. The building was classified with a seismic fortification intensity of 7 degrees (0.15 g) and a designed service life of 50 years. Post-construction, it was observed that the slab's deflection negatively impacted the comfort and load-bearing safety of the residential building. After a comparative analysis of strengthening schemes, the application of CFRP bonding to the underside of the RC two-way slab was selected for strengthening.

CFRP strips were uniformly bonded along the transverse and longitudinal directions on the underside of the slab using an epoxy resin adhesive. The CFRP grade used was I-300, which corresponds to a design tensile strength greater than 3400 MPa (Grade I) and a weight of 300 g/m^2. The CFRP strengthening consisted of a single layer with a thickness of 0.167 mm, a width of 100 mm, and a clear spacing of 100 mm between the strips. The

testing of the CFRP material showed that the average tensile strength was 3500 MPa, complemented by an average elastic modulus of 254 GPa. For the installation of CFRP, the concrete surfaces were meticulously prepared following a standardized procedure. Initially, the surfaces were roughened to enhance adhesion, creating a mechanical key that would secure the epoxy adhesive, followed by thorough cleaning to ensure a robust bond at the interface with a designed bond strength of 4.0 MPa. Subsequently, the CFRP sheets, each 100 mm in width with a clear spacing of 100 mm between strips, were installed with precision. Between 15 and 30 min post-initial application, a second layer of epoxy was applied to foster significant chemical bonding, a critical method for withstanding shear stresses that are inherent to the structure's service life. The curing period for the strengthened RC slabs, inclusive of the CFRP sheets and the epoxy resin, spanned a full seven days after the strengthening system's application. Further, this curing process necessitated the maintenance of specific temperature and humidity conditions to guarantee the proper curing of the resin. The implementation of the strengthening scheme and the in situ arrangement are captured in Figure 1.

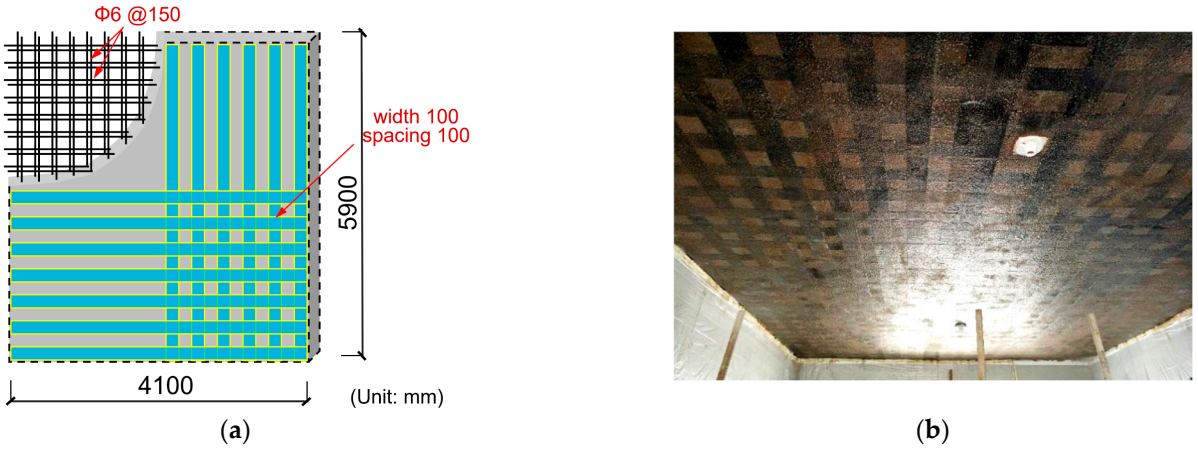


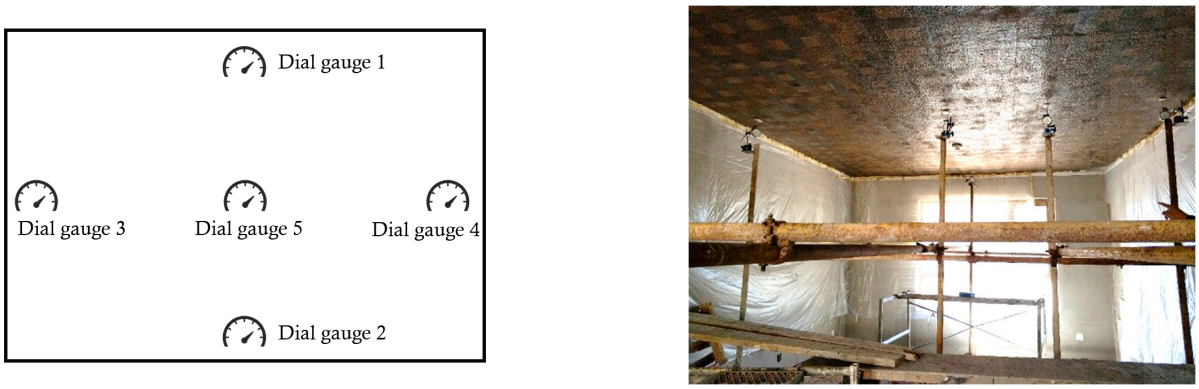
Figure 1. CFRP-strengthening on the underside of the two-way slab; (**a**) Construction details; (**b**) Post-construction condition.

The two-way slab specimens involved in the experimental analysis exhibited initial defects in deflection. Each slab's initial defect was marked by mid-span deflection. Being precast composite slabs, they were noted to have frequent water ponding at the center of the upper surface following the placement of a site-cast layer and the curing process. Using a gradienter to measure the deformation of each slab's upper or lower surfaces, it was confirmed that the mid-span deflection reached a stable value of 12 mm. To ensure that their load-carrying and deformation capacities meet the requirements during the subsequent normal use phase of the structure, the slabs were strengthened by evenly spacing and fully adhering CFRP strips to the lower surface. Considering that the RC two-way slab had already been cast and that it was necessary to conduct performance testing of structural components in accordance with the requirements of the "Code for Acceptance of Construction Quality of Concrete Structures" [38], a stepwise loading test was conducted at a safe level to assess and evaluate the effectiveness of the strengthening measures. The test response of the two-way slab under load was utilized to appraise the structural strengthening outcomes.

2.2. Testing Method

The load test was conducted to assess the safety of the slab under the quasi-permanent combination (QC) of loads, including the detection of cracks at the underside of the slab and mid-span deflections, as well as under the basic combination (BC) of loads (design

loads). For the purpose of crack detection, a thorough flashlight inspection was performed on the underside of the slab, focusing on critical areas such as the central region, the vicinity of diagonals, and the perimeter to scrutinize the spaces between CFRP strips for the occurrence or propagation of concrete cracks. During the loading test, scaffolding was erected at the underside of the slab, and five dial gauges were installed in groups to collect vertical deformation values at different locations, as shown in Figure 2. To ensure the consistency of data monitoring throughout the prolonged experimental period, mechanical dial gauges were utilized. Meticulous attention was devoted to minimizing any disruptions to the gauges during both data acquisition and observational phases, thereby guaranteeing the precision and dependability of the data collected.



(**a**) (**b**)

Figure 2. Dial gauges layout under the RC slab; (**a**) Schematic diagram; (**b**) Construction layout.

The self-weight of the two-way slab, G_{1k}, is 4.0 kN/m^2; the self-weight of the concrete post-pouring layer, G_{2k}, is 1.2 kN/m^2; and the live load, Q_k, is 2.0 kN/m^2 [39].

(1) Load on QC stage:

The total load of the slab is:

$$Q_s = G_{1k} + G_{2k} + 0.4Q_k = 6.0 \text{ kN/m}^2 \quad (1)$$

The loading weight for the quasi-permanent load combination is determined by deducting the self-weight G_{1k} from the load value:

$$W_{QC} = (Q_s - G_{1k})S_0 = 47.4 \text{ kN} \quad (2)$$

In the formula, S_0 represents the net area of the slab component, and it is calculated that S_0 is 23.69 m^2.

(2) Load on BC stage:

$$Q_d = 1.2(G_{1k} + G_{2k}) + 1.4Q_k = 9.04 \text{ kN/m}^2 \quad (3)$$

$$W_{BC} = (Q_d - G_{1k})S_0 = 119.40 \text{ kN} \quad (4)$$

Combined with Equations (3) and (4), it is calculated that W_{BC} is 119.40 kN.

2.3. Multi-Stage Loading

Upon completing the load combination calculations, it was ascertained that the loading process would be bifurcated into two distinct phases, designated QC and BC, encompassing a total of nine distinct levels, culminating in a cumulative load of 119.4 kN. In the execution of in situ testing and loading procedures, 25 kg sandbags were strategically

employed to incrementally apply the load. At the onset of each loading stage, the precise number of sandbags was determined in accordance with the pre-calculated load specifications. Throughout the loading phase, a lightweight engineer carefully placed the sandbags across the floor, ensuring a uniform and stable distribution, thus mitigating any potential adverse effects from the loading activities. The initial phase, QC, was dedicated to the scrutiny of cracks and deflections and was executed in four progressive increments. Each increment was calibrated at 0.5 kN/m², with the initial three increments maintained for a duration of approximately 5 to 10 min and the final increment sustained for approximately 30 min; at each loading tier, deflections and crack widths were meticulously measured. A comprehensive illustration of the loading increments is presented in Figure 3.



(**a**) Level 1 (**b**) Level 2 (**c**) Level 3 (**d**) Level 4

Figure 3. Load increments at stage QC.

The second phase, designated the BC stage, focuses on the inspection of cracks and deflections. This phase was carried out in five increments, with each increment loading at a determined weight of 0.6 kN/m^2. Consistent with the QC stage, the first four increments were maintained for a period of approximately 5 to 10 min, whereas the ultimate increment was held for around 30 min. During this phase, close attention was paid to any indications of structural failure. A detailed depiction of the loading increments is provided in Figure 4. The corresponding deflections of the mid-span of the slab in each load increment are listed in Table 1.



(**a**) Level 5 (**b**) Level 6 (**c**) Level 7

(**d**) Level 8 (**e**) Level 9

Figure 4. Load increments at stage BC.

Table 1. Multi-stage loading and the corresponding deflections.

Load Stage	Load Increment (kN/m^2)	Load in Total (kN)	Mid-Span Deflection (mm)
Level 1	0.50	11.85	0.11
Level 2	0.50	23.70	0.24
Level 3	0.50	35.55	0.42

Table 1. *Cont.*

Load Stage	Load Increment (kN/m^2)	Load in Total (kN)	Mid-Span Deflection (mm)
Level 4	0.50	47.40	0.53
Level 5	0.60	61.60	0.71
Level 6	0.60	75.80	0.91
Level 7	0.60	90.00	1.11
Level 8	0.60	104.25	1.39
Level 9	0.65	119.60	1.64

2.4. Testing Result

Upon completion of each increment of the load in the two stages, the underside of the slab was inspected for any signs of concrete cracking, and the CFRP was examined for signs of tensile rupture or adhesive failure. Observations revealed that after the ninth level of load application, the mid-span deflection of the slab increased gradually, yet no concrete cracking, debonding, or tearing of the CFRP-strengthened slab was observed. These experimental findings indicate that the load-bearing capacity of the two-way slab strengthened with bonded CFRP is reliable and meets the standards for normal structural use. However, the impact of the strengthening treatment on the ultimate strength of the slab requires further validation through numerical simulation.

3. FE Modelling

3.1. Simulation Set-Up

In conducting an ABAQUS FE analysis of CFRP-strengthened concrete two-way slabs with bonded CFRP, the epoxy adhesive used was shown to provide effective bonding after surface treatment, as indicated by material property tests. Consequently, it was assumed that the adhesion between the CFRP and the concrete was sound, with no relative slippage occurring, and the "tie" contact was applied to simulate the bonding effect of CFRP. Additionally, given the CFRP's negligible thickness of only 0.167 mm in the model, its thickness was disregarded in the calculations, treating it as a thin film closely adhering to the underside of the two-way slab.

The concrete material was selected as a damage plasticity model [40], with the stress–strain relationships for compression and tension modes depicted in Figure 5. To enhance computational efficiency, the constitutive relationship for the steel material was modeled using a bilinear ideal elastoplastic model. The CFRP was characterized by a linear elastic criterion, with material failure occurring when the tensile stress exceeded the tensile strength. In the FE model, the materials were defined by different values tested in a laboratory, with the parameters listed in Table 2.

Table 2. Materials' performance in the laboratory.

Material	Grade	Sectional Dimension (mm)	Strength (MPa)	SD. (MPa)	Elastic Modulus (10^5 MPa)
Concrete	C25	160.81	28.7 (compression)	3.19	0.29
Steel	CRB600H	6.02	527.3 (yield stress)	19.76	2.09
CFRP	I-300	0.167	3512.7 (tension)	9.75	2.54

For the finite element simulation, the mesh type selection was as follows: twenty-node quadratic reduced integration hexahedral element (C3D20R) was used for concrete components, three-node quadratic integration three-dimensional truss element (T3D3) was applied for CFRP-strengthened components, and eight-node reduced integration shell element (S8R) was utilized for CFRP components. After several trial calculations, the

element dimensions for each component were approximately discretized to a range of 30 to 50 mm, ensuring a balance between accuracy and computational efficiency.

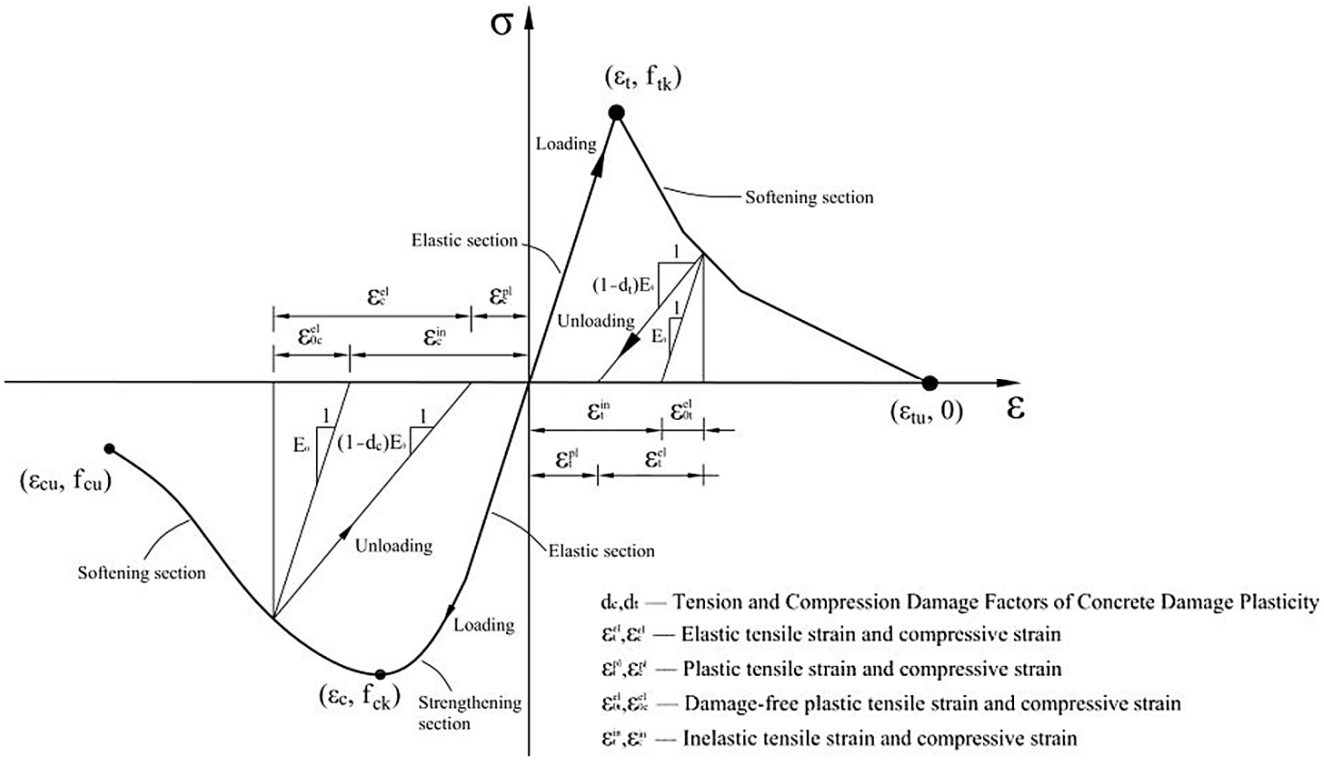


Figure 5. Constitutive curve of the concrete-damaged plasticity model.

3.2. Boundary and Loading Conditions

To accurately simulate the structural support conditions and loading characteristics that a two-way slab would experience under real-world service conditions, it was noted that negative bending moments were present at the slab's edges during the loading process. Consequently, the boundary constraints for the slab in the simulation were modeled as fully fixed to reflect these conditions.

Additionally, to enhance computational accuracy during the loading phase, several measures were implemented. These included refining the mesh to improve the resolution of the model, utilizing element types that employ quadratic interpolation functions for a more accurate representation of material behavior. While the refinements significantly increased the computational load, the structural form, boundary conditions, and loading modes of the problem exhibited ideal symmetry.

Given this symmetry, this study adopted a semi-modeling optimization method for the structure. This approach involved creating a model that represents only a portion of the structure, leveraging the symmetry to reduce the computational domain. This simplified modeling technique ensured that the computational results met the necessary accuracy requirements while also achieving a reduction in computational complexity and an increase in simulation efficiency. Figure 6 provides a visual representation of the quarter model, with the total load applied within the model constituting a quarter of the total structural load. During post-processing, to obtain the reaction forces from the quarter model that correspond to the full structure, the extracted values must be multiplied by 4 to achieve the correct scaling. The upper right portion of the figure illustrates the doubly reinforced two-way slab structure that was included in the calculations, while the lower part demonstrates the layout of the CFRP after symmetric restoration.

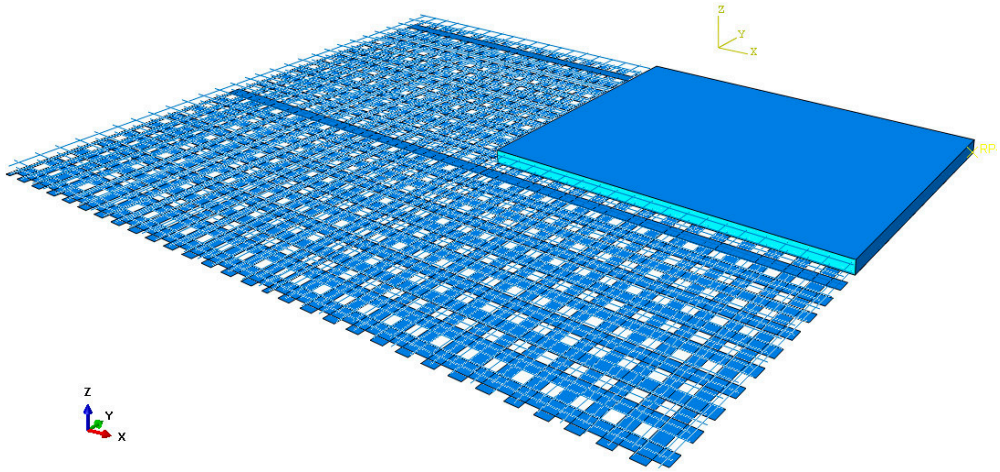


Figure 6. Quarter model simplification of CFRP-strengthened slab in ABAQUS.

The loading process was meticulously executed by configuring ten standardized analysis steps within the model. In the first analysis step, a uniform load was applied until the mid-span deflection of the slab matched the initial deflection of the original two-way slab component, simulating the initial deformation. It is noteworthy that during this step, the interaction of the CFRP elements was temporarily deactivated until the two-way slab reached a pre-defined downward deflection. During this phase, the CFRP elements were not engaged in load-bearing, allowing only the CFRP-strengthened concrete two-way slab to undergo deformation. Once the slab achieved the preset deflection, the CFRP elements were reactivated in the subsequent analysis steps to participate in the load-bearing process and to actualize their strengthening effect.

The remaining nine analysis steps systematically applied the test load values, as detailed in Figure 7, to further evaluate the slab's response to increasing loads and to assess the effectiveness of CFRP-strengthened in enhancing the load-bearing capacity and structural performance of the two-way slab. This structured approach ensured a comprehensive analysis of the slab's behavior under simulated service conditions, providing valuable insights into the CFRP-strengthened strategy's efficacy.

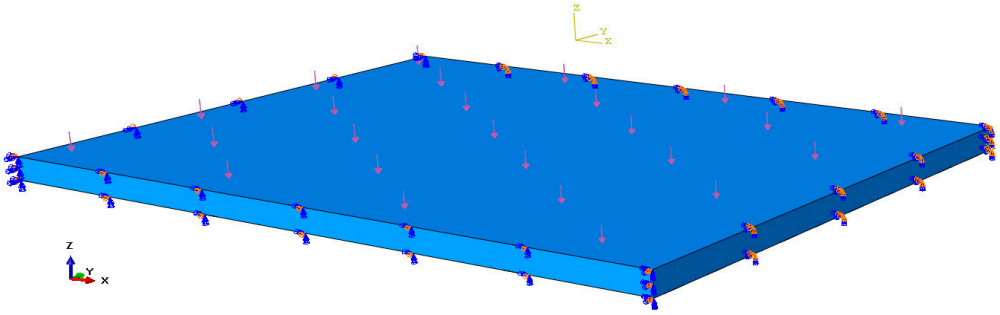


Figure 7. Constraints and loading of computing model.

4. FE Results

During the incremental loading process, observations were recorded at each stage for the lower surface of the slab. The deflection values from the in situ load test were recorded by the dial gauges, and the numerical simulation results were analyzed using data that stabilized after multiple mesh refinements. Table 3 presents a comparison of mid-span deflection values. After subjecting the slab to nine levels of loading, no concrete cracking or CFRP debonding failure was observed at the underside of the slab, and no load-bearing failure was apparent. The finite element analysis (FEA) results were consistent with the test

results, and there were no component failures due to material yielding or contact failure that terminated the calculation. The deflection comparison data presented in the table reveal that the calculated values closely correspond with the measured data, which underscores the reliability and precision of the FEA method. This alignment between the numerical predictions and the empirical observations validates the FEA as a dependable tool for predicting the structural behavior of CFRP-strengthened concrete slabs strengthened with CFRP under loading conditions.

Table 3. Deflection comparison of load test and FEA of two-way slab.

Load Stage	Mid-Span Deflection (mm)	FEA Deflection (mm)	Error
Level 1	0.11	0.15	0.36
Level 2	0.24	0.29	0.21
Level 3	0.42	0.44	0.05
Level 4	0.53	0.59	0.11
Level 5	0.71	0.78	0.10
Level 6	0.91	0.97	0.07
Level 7	1.11	1.15	0.04
Level 8	1.39	1.34	−0.04
Level 9	1.64	1.53	−0.07

Figure 8 illustrates a graded statistical analysis of the deflection of the two-way slab. The simulated data accurately reflected the test results of the in situ experiment. The proximity of the two curves is related to the fact that the concrete, steel reinforcement, and CFRP materials were still in the elastic phase of loading during the testing phase. Upon comparison of the load–deflection curves of various models, it was observed that the model of the two-way slab without CFRP-strengthening showed a mid-span deflection approximately 50% greater than that of the CFRP-strengthened slab model under the same load. Although the mid-span deflections were all below 3 mm, the strengthening effect of the bonded CFRP was further demonstrated through a more detailed comparison.

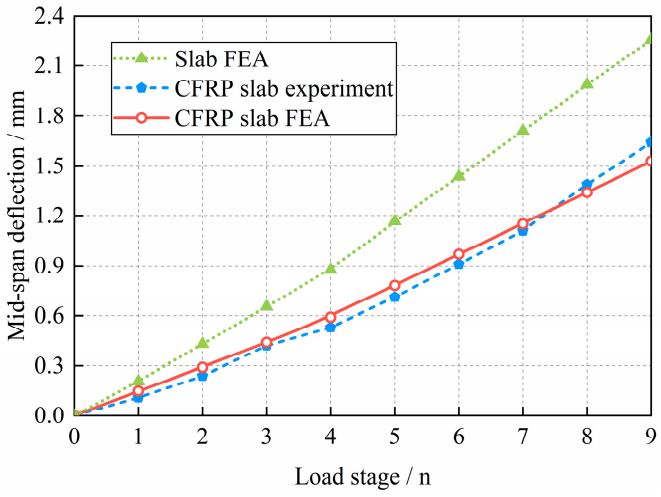


Figure 8. Load–deflection curve comparison between experimental and FEA result.

Figure 9 depicts the distribution of von Mises stress within the concrete and CFRP elements during the loading process. The stress contour plot revealed that the CFRP actively participated in load-bearing during the experiment, effectively sharing the load with the RC slab. The stress contour plot revealed that the CFRP actively participated in load-bearing throughout the test, efficiently sharing the load with the RC slab. This led to a more uniform distribution of stress across the concrete slab, with Mises stress values roughly remaining

below 24.14 MPa. Notably, the stress values in the edge regions, which experienced a combination of bending and shear forces, were less than 3.45 MPa. In contrast, the stress within the CFRP was markedly higher, particularly at the anchorage zones. The surface load applied to the upper surface of the slab was effectively transferred to the CFRP, which served to strengthen and enhance the structural capacity of the component. The analysis results indicated that the stress was primarily concentrated at the anchorage edges of the CFRP and at mid-span areas where the strain was relatively high. The numerical simulation results accurately reflected the actual stress mechanisms, demonstrating the effectiveness of CFRP in reinforcing and strengthening the structural integrity of the slab.

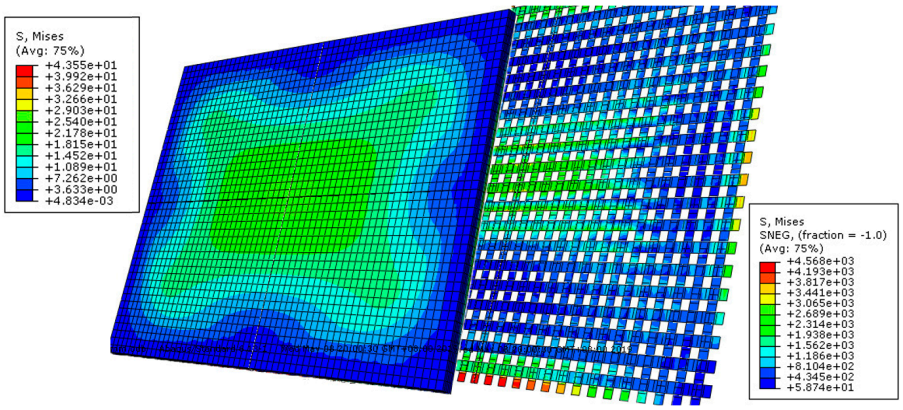
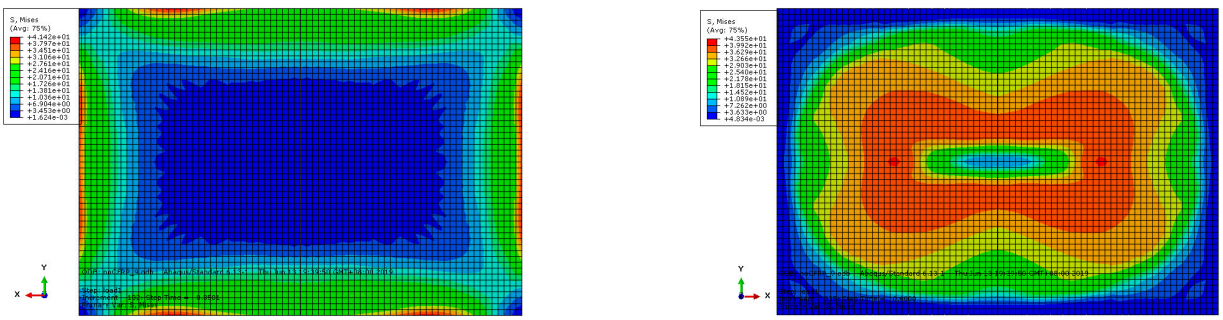


Figure 9. Stress contour plot of concrete and CFRP at loading stage Level 7.

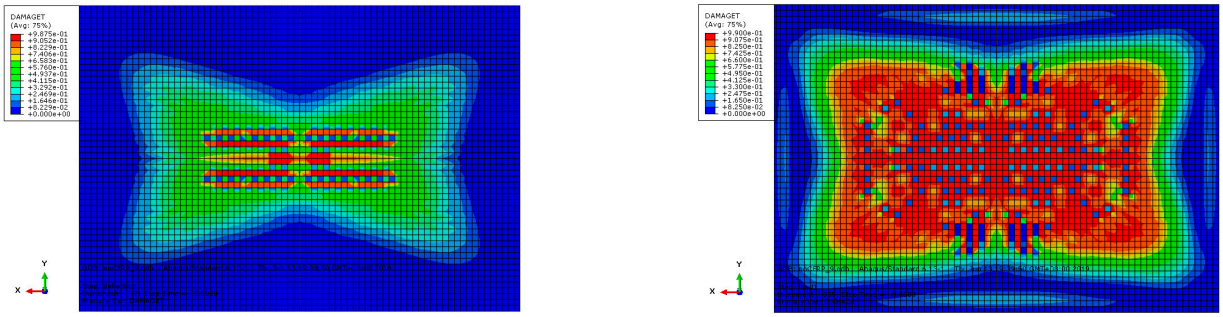
In order to substantiate the enhancement of the load-bearing capacity of the two-way slab attributable to the CFRP-strengthened strategy, a numerical simulation was utilized to simulate an ultimate loading experiment. This simulation facilitated a comparative analysis of the stress values on both the lower and upper surfaces of the slab, with a focus on the CFRP-strengthened conditions, across the entire loading process. The objective was to evaluate the ultimate load-bearing capability and the deformation characteristics at the yield point of the specimens, as well as to ascertain the degree of improvement of the slabs strengthened with CFRP. Figure 10 depicts the stress distribution within the concrete section of the two-way slab. It is evident from the figure that in the absence of strengthening, the slab experiences elevated stress concentrations along the 45-degree diagonals at the lower surface, within the support boundary regions, and around the circumference of the central area on the upper surface. These stress concentrations are indicative of areas that are prone to cracking or crushing under load, underscoring the importance of CFRP-strengthening in such critical structural components.



(**a**) lower surface (**b**) Upper surface

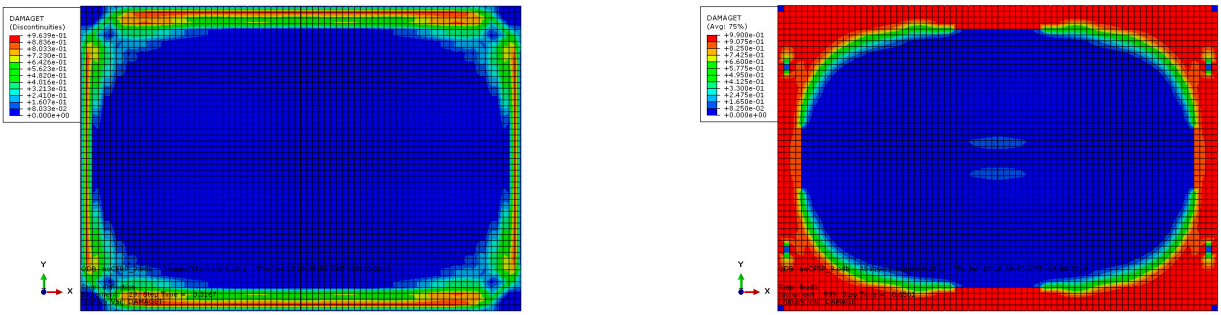
Figure 10. Stress contour plots of the unstrengthened slab.

The tensile damage contour plots of the concrete in the unstrengthened slab are depicted in Figures 11 and 12. It was observed that from the first (Level 4) to the second (Level 9) phase, the damaged areas evolved and spread, with significant tensile failure in the concrete at the mid-span underside of the slab and the constrained boundary areas on the upper surface, where cracking was notably pronounced. The distribution of tensile damage in the lower concrete surface of the unstrengthened slab, as reflected by the DAMAGET factor, escalated from a limited area exceeding 0.75 in Figure 11a to nearly 70% of the area with values exceeding 0.8 in Figure 11b. A similar consistent pattern is observed upon comparison of Figure 12a,b. This observation underscores the essential and critical role of CFRP-strengthening in preventing the propagation of cracks and potential structural failure in these regions.



(**a**) Level 4 (**b**) Level 9

Figure 11. Concrete tensile damage contour plot of lower surface in unstrengthened slab.



(**a**) Level 4 (**b**) Level 9

Figure 12. Concrete tensile damage contour plot of upper surface in unstrengthened slab.

Figure 13 illustrates the steel stress distribution within the doubly reinforced slab. The stress contour plot of the steel correlates with the stress and failure patterns observed in the concrete of the slab. It was analyzed that in the unstrengthened slab, CFRP-strengthening played a crucial role in bearing a portion of the load and in limiting excessive deformation at the mid-span. The stress contour revealed that the concrete stress values were notably higher at the 45-degree diagonals and the support boundary areas on the lower surface of the slab, as well as within the circumferential range at the center of the upper surface, where cracks or crushing phenomena in the concrete were likely to occur under load.

The comparison of the stress contour plots revealed that after strengthening with CFRP, the stress levels in the concrete were significantly lower under the same loading stage, as depicted in Figure 14. The lower surface of the strengthened slab displayed a notably uniform distribution of stress, reaching a peak of 19.76 MPa, whereas the upper surface experienced maximum compressive stress of 24.70 MPa, with the high-stress region notably localized to a narrow area at the slab's mid-span. Simulation during the ultimate load stage indicated that the stress in the CFRP strips (as shown in Figure 15) was approximately an order of magnitude higher than the tensile stress in the concrete. The synergistic

action of CFRP and steel reinforcement enhanced the ultimate load-bearing capacity and deformation capacity of the two-way slab, thereby increasing the safety margin of the structural component. The comparison of the stress data between the strengthened and unstrengthened slabs demonstrated the substantial enhancement in load-bearing capacity achieved through the application of CFRP-strengthening. CFRP-strengthening not only increased the overall strength of the slab but also helped to distribute the stress more evenly, reducing the concentration of stress in critical areas and thereby delaying the onset of cracking or crushing.

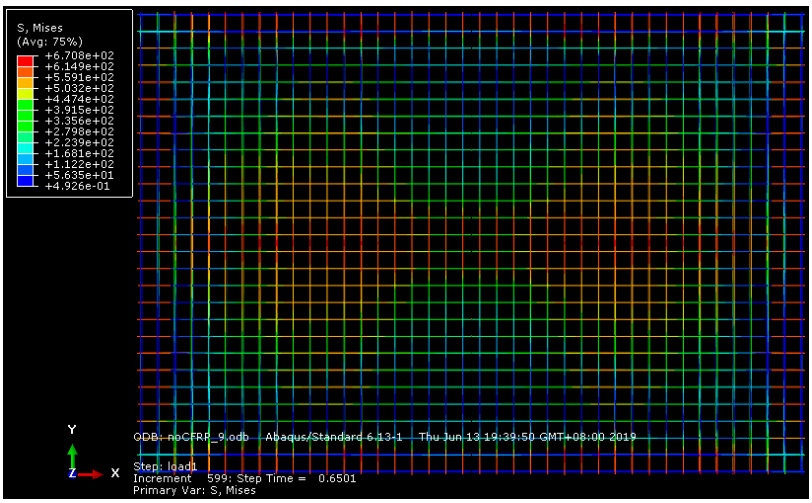
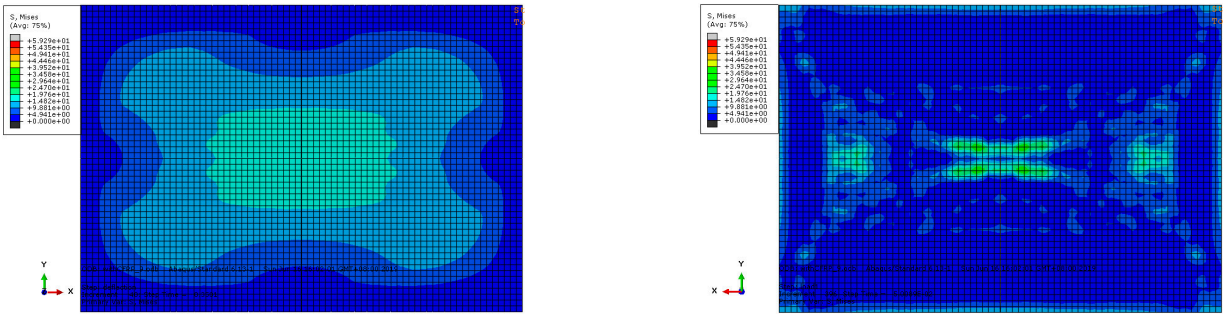


Figure 13. Mises stress contour plot of steel in the unstrengthened slab.



(**a**) lower surface (**b**) Upper surface

Figure 14. Stress contour plot of the CFRP-strengthened slab.

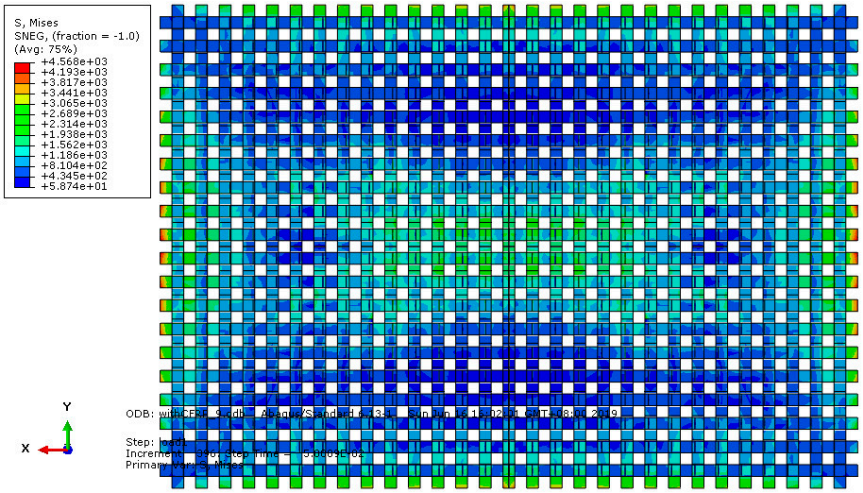


Figure 15. Stress contour plot of CFRP of the strengthened slab.

The yielding of the component was defined by the experimental deflection reaching 1/50 of the span (approximately 120 mm). Figure 16 illustrates the load–displacement curve of the slab component. At the yielding point of the unstrengthened two-way slab, the load capacity was 95 kN/m^2. Post-yielding, the component's load capacity could not increase further, and the deflection rapidly increased, leading to complete failure of the slab. In contrast, the slab strengthened with CFRP could withstand a load of 135 kN/m^2 when the deflection reached 120 mm, and the load capacity could further increase to 140~150 kN/m^2 after yielding. The ultimate load capacity was approximately 50% higher than that of the unstrengthened contrast model. The comparative results indicate that the CFRP-strengthened scheme effectively ensured an adequate level of structural safety and security.

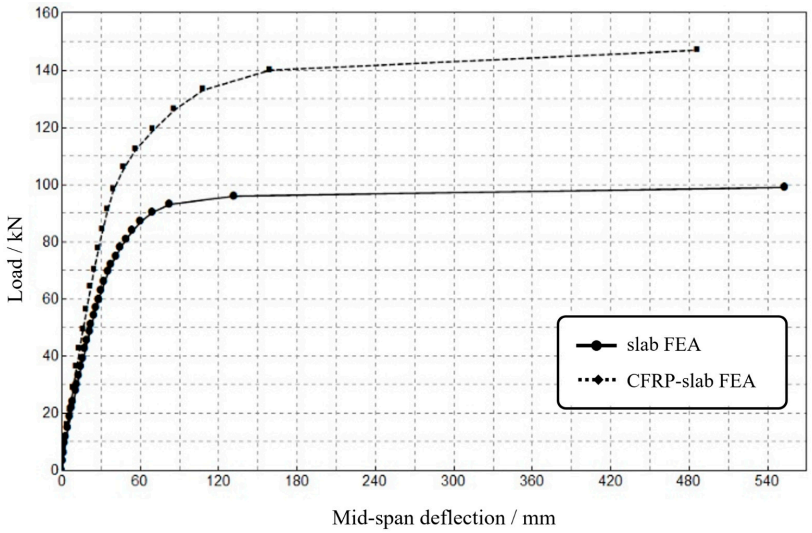


Figure 16. Curve comparison of two-way slabs under ultimate loading experiment.

5. Conclusions

In this paper, an in situ test and FE simulation of the effectiveness of CFRP-strengthening on the load-bearing performance of RC two-way slabs was conducted, utilizing both in situ multi-stage loading experiments and nonlinear FEA. The findings are encapsulated in the conclusions presented below:

(1) The experimental evidence has confirmed that the utilization of CFRP for the strengthening of RC two-way slabs exhibiting an initial defect is a dependable and efficient approach. The strengthening application of CFRP proves to be not only feasible but also highly practical during the construction phase of strengthening. In devising CFRP strengthening strategies, the quantity of CFRP layers and the spacing between them can be meticulously tailored to accommodate the specific geometrical attributes and load-bearing specifications of the component. Such customization enhances the overall efficacy of the strengthening scheme, ensuring an optimized outcome aligned with structural performance objectives.

(2) After effectively simplifying the structure within ABAQUS 6.13 software, the process of CFRP and RC two-way slabs jointly sustaining loads can be accurately simulated by appropriately configuring the finite element properties, material constitutive models, and loading procedures. A comparison of the numerical simulation outcomes with the in situ test results has validated the consistency between the numerical analysis and the experimental data. The final mid-span deflection results exhibited discrepancies of −7% between the simulated calculations and the actual measurements, thereby underscoring the accuracy of the analytical methodology.

(3) Numerical simulation outcomes, including stress and damage contour plots, demonstrate a marked enhancement in the load-bearing capacity of the slab components due to the presence of reinforcement bars and bonded CFRP layers. The slab's underside area, which initially exhibited tensile damage coefficients above 0.8 for concrete in over 70% of its area, has been changed to no signs of tensile or compressive damage on either surface. The simulation's analytical outcomes reveal that CFRP strengthening has significantly enhanced the slab's structural integrity and load-bearing capacity. Additionally, the slabs experience a more uniform distribution of stress, ably shared by the CFRP layers. Simulation calculations have confirmed that the ultimate load capacity of the CFRP-strengthened components has increased by about 50% relative to the unstrengthened component.

Author Contributions: Conceptualization, Y.S.; methodology, Y.S.; software, Y.S. and Y.G.; validation, Y.G.; formal analysis, Y.S.; investigation, Y.S. and Y.G.; resources, Y.S.; data curation, Y.G.; writing—original draft preparation, Y.S.; writing—review and editing, Y.G.; visualization, Y.S. and Y.G.; supervision, Y.G.; project administration, Y.S. and Y.G.; funding acquisition, Y.S. All authors have read and agreed to the published version of the manuscript.

Funding: This research received no external funding.

Data Availability Statement: The data presented in this study are available upon corroborated request from the corresponding author.

Conflicts of Interest: The authors declare no conflicts of interest.

References

1. Buitrago, M.; Adam, J.M.; Moragues, J.J. Load transmission between slabs and shores during the construction of RC building structures—A review. *Eng. Struct.* **2018**, *173*, 951–959. [CrossRef]
2. Mahmoud, H.S.; Hawileh, R.A.; Abdalla, J.A. Strengthening of high strength reinforced concrete thin slabs with CFRP laminates. *Compos. Struct.* **2021**, *275*, 114412. [CrossRef]
3. Mercimek, Ö.; Ghoroubi, R.; Erbaş, Y. Comparison of strengthening methods to improve punching behavior of two-way RC flat slabs. *Structures* **2022**, *46*, 1495–1516. [CrossRef]
4. Shen, J.; Dai, H.; Zhou, G. Shear behavior of pre-damaged RC beams strengthened with UHPFRC-CFRP grid layer. *Compos. Struct.* **2024**, *349–350*, 118520. [CrossRef]
5. Mansour, W.; Li, W.; Ghalla, M. Improving the punching capacity of two-way RC flat slabs via external strengthening using various configurations of aluminum sheets. *Constr. Build. Mater.* **2024**, *420*, 135611. [CrossRef]
6. Aljidda, O.; El Refai, A.; Alnahhal, W. Experimental and numerical investigation of the flexural behavior of one–way RC slabs strengthened with near–surface mounted and externally bonded systems. *Constr. Build. Mater.* **2024**, *421*, 135709. [CrossRef]
7. Hawileh, R.; Douier, K.; Gowrishankar, P. Durability of externally strengthened concrete prisms with CFRP laminates and galvanized steel mesh attached with epoxy adhesives and mortar. *Compos. Part C Open Access* **2024**, *14*, 100493. [CrossRef]
8. Sahranavard, S.; Jahangir, H.; Haji kazemi, H. An experimental and numerical investigation of RC slabs externally strengthened by perforated steel plates. *Structures* **2022**, *45*, 1239–1252. [CrossRef]
9. Oret, G.; Limam, O. Experimental and numerical analysis of RC two-way slabs strengthened with NSM CFRP rods. *Constr. Build. Mater.* **2008**, *22*, 2025–2030.
10. Limam, O.; Nguyen, V.T.; Foret, G. Numerical and experimental analysis of two-way slabs strengthened with CFRP strips. *Eng. Struct.* **2005**, *27*, 841–845. [CrossRef]
11. Jin, L.; Zhang, B.; Chen, F. CFRP-strengthened shear walls: Combined effects of CFRP and reinforcement ratio. *Int. J. Mech. Sci.* **2024**, *282*, 109634. [CrossRef]
12. Li, L.; Chen, J.; Wang, W.T.; Dai, K.Y.; Hu, W.B. Experimental and prediction model of axial compressive responses of corroded RC cylinders strengthened with CFRP. *Eng. Struct.* **2024**, *317*, 118649. [CrossRef]
13. Gholami, M.; Sam, A.R.M.; Yatim, J.M. A review on steel/CFRP strengthening systems focusing environmental performance. *Constr. Build. Mater.* **2013**, *47*, 301–310. [CrossRef]
14. Jung, D.; Kim, K.H.E.; Choi, H. Shear strengthening and damage control effects of CFRP and self-prestressing iron-based SMA for concrete columns. *Compos. Struct.* **2025**, *351*, 118550. [CrossRef]
15. Wang, H.T.; Liu, S.S.; Shi, J.W. Bonded and unbonded strengthening of RC beams with the prestressed CFRP plate system: An experimental study. *Constr. Build. Mater.* **2024**, *438*, 137118. [CrossRef]

16. Elnagar, M.E.; Makhlouf, M.H.; El-sayed, K.M. An experimental and numerical study on two-way RC slabs with openings strengthened by ferrocement technique. *Structures* **2024**, *65*, 106673. [CrossRef]
17. Joyklad, P.; Krishna Gadagamma, C.; Maneengamlert, B. Structural behavior of RC one-way slabs strengthened with ferrocement and FRP composites. *Eng. Fail. Anal.* **2024**, *161*, 108328. [CrossRef]
18. Al-Rousan, R. Performance of reinforced concrete slabs strengthened with different types and configurations of CFRP. *Compos. Part B Eng.* **2012**, *43*, 510–521. [CrossRef]
19. Santos, G.S. Punching CFRP-based strengthening solutions for reinforced concrete flat slabs. *Compos. Struct.* **2019**, *224*, 111077. [CrossRef]
20. Breveglieri, M. RC slabs strengthened with externally bonded CFRP strips under long-term environmental exposure and sustained loading. Part 2: Laboratory experiments. *Compos. Part C Open Access* **2021**, *6*, 100210. [CrossRef]
21. Al-Rousan, R.Z.; Ababneh, A.N.; Bani Hani, M.S. Effect of different anchorage schemes on the flexural behavior of RC slabs strengthened with CFRP sheets. *Constr. Build. Mater.* **2024**, *428*, 136348. [CrossRef]
22. Ghayeb, H.H.; Atea, R.S.; Al-kannoon, M.A.A. Performance of reinforced concrete flat slab strengthened with CFRP for punching shear. *Case Stud. Constr. Mater.* **2023**, *18*, e01801. [CrossRef]
23. Zhou, C. Experimental study on the flexural strengthening of one-way RC slabs with end-buckled and/or externally bonded CFRP sheets. *Eng. Struct.* **2023**, *282*, 115832. [CrossRef]
24. Li, C.; Xian, G. Novel wedge-shaped bond anchorage system for pultruded CFRP plates. *Mater. Structures.* **2018**, *51*, 162. [CrossRef]
25. Ke, L.; Li, Y.; Li, C.; Cheng, Z.; Ma, K.; Zeng, J. Bond Behavior of CFRP-Strengthened Steel Structures and Its Environmental Influence Factors: A Critical Review. *Sustain. Struct.* **2024**, *4*, 000038. [CrossRef]
26. Xian, G.; Zhou, P.; Li, C.; Dong, S.; Du, H.; Tian, J.; Guo, R.; Peng, Z.; Zhang, Z.; He, T. Mechanical Properties Evaluation of Glass Fiber Reinforced Thermoplastic Composite Plate under Combined Bending Loading and Water Immersion. *Constr. Build. Mater.* **2024**, *440*, 137470. [CrossRef]
27. Dong, S.; Zhou, P.; Ning, Z.; Wu, X.; Li, C.; Xian, G. Durability of Carbon- and Glass-Fiber Reinforced Thermoplastic Polymer Composites: A Literature Review. *J. Build. Eng.* **2024**, *98*, 111055. [CrossRef]
28. Tian, L.; Wang, L.; Xian, G. Machine Learning Prediction of Interfacial Bond Strength of FRP Bars with Different Surface Characteristics to Concrete. *Case Stud. Constr. Mater.* **2024**, *21*, e03984. [CrossRef]
29. Ghalla, M.; Badawi, M.; Hu, J.W.; Elsamak, G.; Mlybari, E.A.; Emara, M. Ultimate Performance of Two-Way Reinforced Concrete Flat Slabs Enhanced by SHCC Drop Panels Mitigating Punching Failure. *J. Build. Eng.* **2024**, *99*, 111574. [CrossRef]
30. Abdulrazzaq, M.M.; Hilo, S.J.; Sabih, S.M. Numerical investigation for the flexural load behaviour of profiled composite slab strengthened with CFRP. *Mater. Today Proc.* **2022**, *61*, 1115–1125. [CrossRef]
31. Abas Golham, M.; Al-ahmed, A.H.A. Behavior of GFRP reinforced concrete slabs with openings strengthened by CFRP strips. *Results Eng.* **2023**, *18*, 101033. [CrossRef]
32. Anas, S.M.; Alam, M. Role of shear reinforcements on the punching shear resistance of two-way RC slab subjected to impact loading. In Proceedings of the 13th International Symposium on Plasticity and Impact Mechanics, Chennai, India, 21–26 August 2022; Volume 87, pp. 43–54.
33. Anas, S.M.; Alam, M.; Shariq, M. Behavior of two-way RC slab with different reinforcement orientation layouts of tension steel under drop load impact. In Proceedings of the 13th International Symposium on Plasticity and Impact Mechanics, Chennai, India, 21–26 August 2022; Volume 87, pp. 30–42.
34. Shu, J.; Fall, D.; Plos, M. Development of modelling strategies for two-way RC slabs. *Eng. Struct.* **2015**, *101*, 439–449. [CrossRef]
35. Xu, S.; Xie, H.; Li, Q. Bending performance of RC slabs strengthened by CFRP sheets using sprayed UHTCC as bonding layer: Experimental study and theoretical analysis. *Eng. Struct.* **2023**, *292*, 116575. [CrossRef]
36. Sharaky, I.A.; Elamary, A.S.; Alharthi, Y.M. Experimental and numerical investigation on the flexural performance of RC slabs strengthened with EB/NSM CFRP reinforcement and bonded reinforced HSC layers. *Eng. Struct.* **2023**, *289*, 116338. [CrossRef]
37. Zou, C.; Ibrahim, Z.; Hashim, H. Fatigue performance simulation of reinforced concrete beams externally strengthened with side bonded CFRP sheets. *Eng. Struct.* **2024**, *316*, 118530. [CrossRef]
38. *GB50204-2015*; Code for Acceptance of Construction Quality of Concrete Structures. China Academy of Building Research: Beijing, China; China Architecture & Building Press: Beijing, China, 2015.
39. *GB 50010-2010*; Code for Design of Concrete Structures. China Ministry of Construction: Beijing, China; China Architecture & Building Press: Beijing, China, 2015.
40. Shao, S.; Wu, Y.; Fu, H.; Feng, S.; Zhang, J. Numerical Investigation on the Mechanical Properties of Vault Void Lining and Steel Plate Strengthening. *Materials* **2023**, *16*, 789. [CrossRef]

Disclaimer/Publisher's Note: The statements, opinions and data contained in all publications are solely those of the individual author(s) and contributor(s) and not of MDPI and/or the editor(s). MDPI and/or the editor(s) disclaim responsibility for any injury to people or property resulting from any ideas, methods, instructions or products referred to in the content.